Influence of Temperature on the Pressure Distribution Within Press Pack IGBTs

Erping Deng, *Member, IEEE*, Zhibin Zhao, *Member, IEEE*, Zhongkang Lin, Ronggang Han, and Yongzhang Huang

***Abstract*—Press pack (PP) packaging technology has been applied to insulated-gate bipolar transistors (IGBTs) for high-voltage and high power density applications in recent years. The pressure distribution within PP IGBTs is very important because it affects both the electrical and thermal contact resistances, thermal cycling capability, and short-circuit current rating. Too much pressure will mechanically damage the chip and too little pressure will increase the thermal contact resistance, which eventually leads to chip thermal damage. In this paper, a finite-element multiphysics model cocoupled with an electrical field, thermal field, and mechanical field is proposed to analyze the collector current distribution, pressure distribution, and junction temperature distribution within PP IGBTs. The most important coupling variables, such as electrical and thermal contact resistances, for this cocoupled multiphysics model are calculated or measured by experiment through a single IGBT/fast-recovery diode chip submodule. Based on this multiphysics model, the influence of the high temperature generated by the chip's power dissipation on the pressure distribution within PP IGBTs (in the heating phase) is discussed, and then, compared with the pressure distribution in the clamping phase. The results show that the pressure distribution within PP IGBTs in the heating phase is extremely uneven and different from the value in the clamping phase. Furthermore, the mechanical model and its boundary conditions are verified through the pressure distribution experimental results in the clamping phase, which is measured based on the Fuji prescale film and the clamping test bench. Based on the simulation and experimental results, an optimization of the collector electrode and pedestal is proposed to improve the pressure distribution within PP IGBTs in the heating phase.**

***Index Terms*—Current distribution, press pack insulated-gate bipolar transistors (PP IGBTs), pressure distribution, temperature, temperature distribution.**

Manuscript received March 3, 2017; revised May 18, 2017 and August 1, 2017; accepted September 2, 2017. Date of publication September 5, 2017; date of current version March 5, 2018. This work was supported in part by the National Natural Science Foundation of China 51477048 and in part by the National Key R&D Program of China 2016YFB0901800. Recommended for publication by Associate Editor X. Wu. *(Corresponding author: Erping Deng.)*

E. Deng is with the State Key Laboratory of Alternate Electrical Power System With Renewable Energy Sources, North China Electric Power University, Beijing 102206, China, and also with the Global Energy Interconnection Research Institute, State Grid Corporation of China, Beijing 102211, China (e-mail: dengerpinghit@163.com).

Z. Zhao and Y. Huang are with the State Key Laboratory of Alternate Electrical Power System With Renewable Energy Sources, North China Electric Power University, Beijing 102206, China (e-mail: zhibinzhao@126.com; huang_yz@ncepu.edu.cn).

Z. Lin and R. Han are with the Global Energy Interconnection Research Institute, State Grid Corporation of China, Beijing 102211, China (e-mail: lzk007x@163.com; salu2134@163.com).

Color versions of one or more of the figures in this paper are available online at http://ieeexplore.ieee.org.

Digital Object Identifier 10.1109/TPEL.2017.2749521

I. Introduction

TO MEET the growing requirements of insulated-gate bipolar transistor (IGBT) device applications, their capacity and reliability have become great challenges. Press pack IGBTs (PP IGBTs) have gradually been applied to high-voltage and high power density applications, such as electric locomotives and high-voltage direct-current transmission, because of their higher reliability, double-side cooling, higher power density, and ease of connection in series [1] compared to typically wire-bonded IGBT modules. The PP packaging style for high-voltage and high power density IGBT can be divided into PP and StakPak. The StakPak packaging style is patent protected by ABB and the research on the StakPak is very limited. The PP is widely used by Poseico, Fuji, Westcode, and Toshiba because of the experience with the packaging of high-power devices, such as gate turn-off thyristors, diodes, etc. [2], and many researches are based on this packaging style. Therefore, the schematic diagram of the PP IGBT studied in this paper is shown in Fig. 1. We can see that it has a multilayered structure. The electrical and thermal paths for the silicon chips are supplied by the collector and emitter copper electrodes. Furthermore, the needed clamping force is also applied on the two electrodes. A silicon chip subassembly is consisted of a silver shim plate, together with a silicon chip and two molybdenum plates [3]. Two molybdenum plates surrounded the silicon chips are used to uniform the clamping force distribution and reduce the thermal expansion/contraction between the molybdenum plates and silicon chips when the PP IGBT undergoes high-temperature variations. Many silicon chip subassemblies connected in parallel to form a PP IGBT and the current rating is determined by its paralleled number. An external clamping force is required to maintain the electrical and thermal contacts of all of the components within PP IGBTs. According to the mounting instructions from the PP IGBT manufacturers, such as ABB [4] and Westcode [5], a pressure of approximately 1.2 kN/ cm^2 is ideal for PP IGBTs.

The research on the pressure distribution within PP IGBTs, especially the influence of temperature on the pressure distribution, is limited. Pirondi *et al.* analyzed the thermomechanical behavior of PP IGBTs during the initial assembly and subsequent uniform thermal cycling through the finite-element method (FEM) in 1998 [6]. The pressure distribution within PP IGBTs under different conditions, for example, the dimensional tolerances, thermal cycling, is analyzed. However, this thermomechanical model is not accurate enough because the thermal contact resistance is not included and no experimental results are

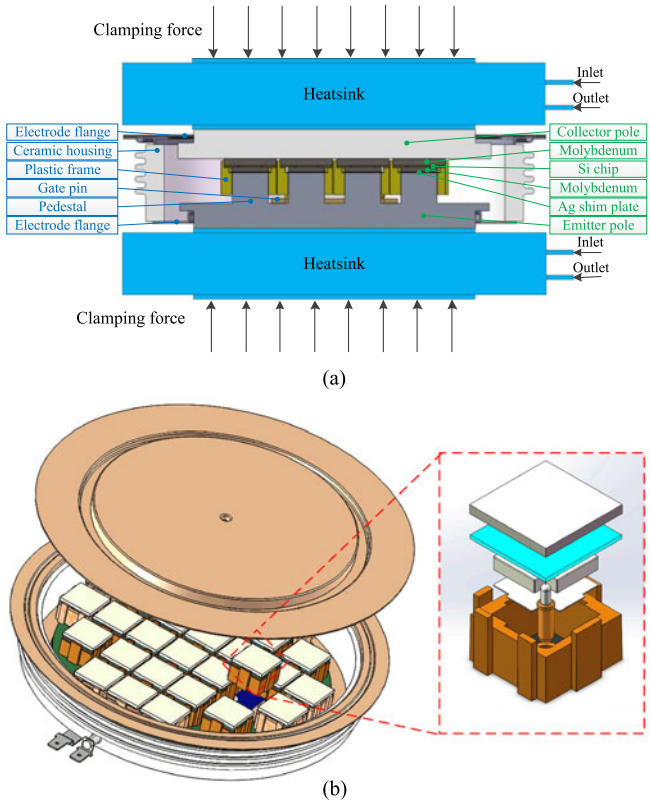

Fig. 1. Schematic diagram of PP IGBTs. (a) Section view. (b) Exploded view.

used to verify it. Cova *et al*. also analyzed the thermomechanical behavior and developed a testing rig for accelerated testing of a single chip in 1999 [7]. The failure prediction based on this test bench and thermomechanical model is also performed. Poller *et al*. proposed a multiphysics model to discuss the temperature and pressure distributions within PP IGBTs in the power cycling phase in 2012 [8], and then, discussed the influence of the clamping force on the collector current, temperature, and pressure distribution in 2013 [9] using FEM simulations. The simulation results show that the clamping conditions affect the current, temperature, and pressure distributions, and, furthermore, the high temperature also has an important influence on the pressure distribution compared with the clamping phase. However, the power dissipation model is not accurate enough for the input of the thermal model and the influence of the junction temperature on the power dissipation is not concluded in the proposed multiphysics model. Hasmasan *et al*. also analyzed the influence of the clamping conditions on the collector current, temperature, and pressure distributions in 2013 through a multiphysics model [3]. This literature also shows that the clamping conditions affect the collector current, temperature, and pressure distributions within PP IGBTs, especially the variation in the thickness of the chip assemblies. The clamping force reduces when the chip assembly is reduced by 0.5 μm. This reduction leads to a reduction in the collector current and an increment in the junction temperature because of the electrical and thermal contact resistances. In the same way, the influence of the junction temperature on the power dissipation is not considered

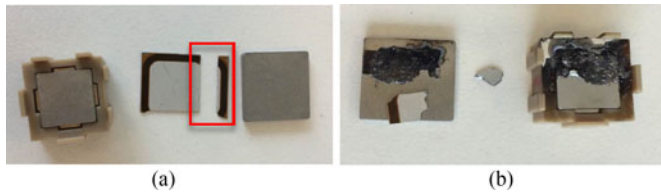

Fig. 2. Failed chips from the nonuniform pressure distribution. (a) Too much pressure. (b) Too little pressure.

in this model. Furthermore, the influence of the junction temperature on the mechanical field is also ignored. Therefore, the two aforementioned multiphysics models are one-way coupled model not the strictly cocoupled model.

The pressure distribution within PP IGBTs is extremely important because it not only affects the electrical contact resistance but also the thermal contact resistance [10]. Then, both the electrical and thermal contact resistances further impact the current and temperature distributions [3]. Furthermore, the pressure distribution within PP IGBTs also affects the reliability. The pictures shown in Fig. 2 are the failed chips from our experiment, which failed as a result of the nonuniform pressure distribution. Too much pressure will mechanically damage the chip and too little pressure will increase the thermal contact resistance. Then, an augmentation of the thermal contact resistance increases the junction temperature, which eventually leads to chip thermal damage. Meanwhile, the pressure distribution within PP IGBTs is also influenced by the temperature distribution. Thus, a multiphysics model that can accurate reflect the electrical, thermal, and mechanical behaviors of PP IGBTs is extremely important.

In order to predict the collector current, temperature, and pressure distributions within PP IGBTs and the influence of high temperature on the pressure distribution accurately, a directly cocoupled multiphysics model is proposed in this paper. It is different with the one-way coupled model that all the fields are coupled with each other. For example, the mechanical field is coupled with the electrical and thermal fields through the electrical and thermal contact resistances, and then, the thermal field is also coupled with the electrical and mechanical fields. In the one-way coupled model, the simulation results are not accurate enough when the coupling relationship between the two fields are very strong. For example, the electrical field coupled with the thermal field which only the power dissipation from electrical field affects the junction temperature from thermal field. Actually the junction temperature of silicon chips affects its electrical characteristic (e.g., the saturation voltage drop of IGBT chip) a lot and then influences the power dissipation. This leads to a junction temperature change in the thermal field again. Therefore, the one-way coupled model underestimate the junction temperature and its distribution within PP IGBT. The cocoupled multiphysics model is much more suitable and accurate for the packaging design of PP IGBTs. The most important coupling parameters for this cocoupled model are the electrical and thermal contact resistances. Both the electrical and thermal contact resistances within PP IGBTs are calculated through the FEM model or measured by experiment. Additionally, the

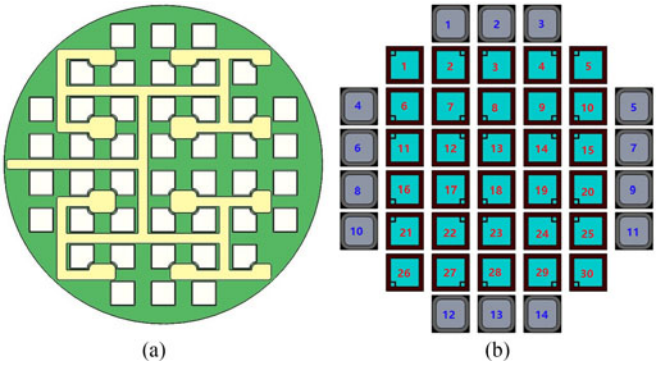

Fig. 3. Conceptual PP IGBT studied in this paper. (a) Internal structure. (b) Chip numbers of the studied PP IGBT.

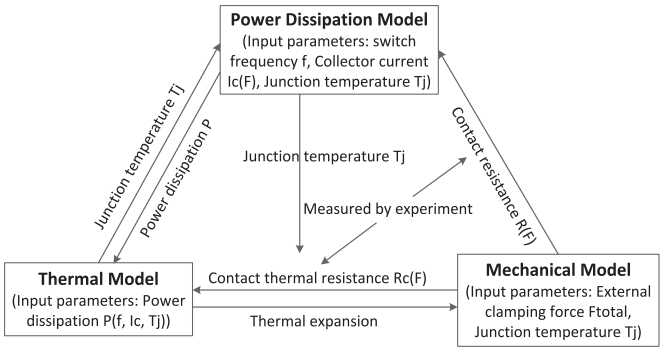

Fig. 4. Multiphysics model of PP IGBTs.

results of the FEM model are verified by the experimental results. The relationship between the contact resistance and clamping force is evaluated to couple the electric and thermal fields with the mechanical field. The power dissipation model is proposed to calculate the power dissipation of the IGBT and fast-recovery diode (FRD) chips, which is also influenced by the junction temperature of the thermal model. Furthermore, the power dissipation is determined by the collector current, which is influenced by the clamping force from the mechanical model. Thus, a FEM multiphysics model that is fully coupled with the electric, thermal, and mechanical fields is proposed to simulate the current, temperature, and pressure distributions.

II. Finite-Element Model

The internal structure and chip numbers of the conceptual PP IGBT, which consist of 30 IGBT chips with 14 antiparalleled FRD chips, are shown in Fig. 3. The IGBT and FRD chips are numbered in red and blue, respectively. Groves are shaped into the pedestals on the emitter side for the gate pin of the housing. The silver plates are not considered in the FEM model in this paper because they are very thin compared with other components and their effect on the pressure distribution is negligible [3].

The physics field in PP IGBTs is extremely complex because it is coupled with the electrical, thermal, and mechanical fields. The multiphysics model of PP IGBTs shown in Fig. 4 is proposed in this paper to analyze the pressure distribution within PP IGBTs. Temperature is the key parameter in the physics field because it affects both the electrical and mechanical characteristics. The switch frequency of the silicon IGBT chip, collector current, and junction temperature are the key parameters that affect the power dissipation in the power dissipation model. The most important parameters that impact the junction temperature in the thermal model are the power dissipation, internal structure of the studied PP IGBT, and heat dissipation conditions. The pressure distribution in the mechanical model is mainly influenced by the external clamping force conditions and thermal stress generated by the high temperature of IGBT chips. In this paper, the variables contributing to the physics fields were coupled together and clearly described. The power dissipation, thermal, and mechanical models are calculated simultaneously, that is to say the physics variables of those models are changed online during the simulation. This is a directly co-coupled multiphysics model for PP IGBTs. Furthermore, the geometry of the packaging components will not influence this multiphysics model because the thermal and mechanical models are 3-D and the interactive effect is included in this model. Meanwhile, the power dissipation model is independent of the geometry of the components. It may change the parameters of this multiphysics model, especially the coupling variables, but will not change the modeling process and this model. For example, the pad size, thickness of the molybdenum layer will change the electrical and thermal contact resistances and then influence the simulation results.

A. Power Dissipation Model

The power dissipation of the IGBT and FRD chips consists of conduction loss and switch loss and can be obtained by experimental measurement or calculation based on the datasheet. In this paper, calculation formulas based on the datasheet will be introduced because the main focus is on the analysis of the temperature distribution instead of the accuracy of the calculated temperature. The total average power dissipation in each IGBT chip is estimated in a simple way using (1) and (2) [11]. The conduction loss of the IGBT chip mainly depends on the collector current, voltage drop between the collector and emitter, power factor, etc. The switch loss mostly relies on the switch frequency, with the assumption that the turn-on and turn-off energies are maintained as constant in every switch process. In the same way, the power dissipation in each FRD chip can be obtained using (3) and (4)

$$P_{\mathrm{cond\_}I} = \sqrt{2} I_{\mathrm{c}} \cdot V_{ce} \cdot \left(\frac{1}{2\pi} + \frac{M\cos\varphi}{8}\right) + 2I_c^2 \cdot r_{ce} \cdot \left(\frac{1}{8} + \frac{M\cos\varphi}{3\pi}\right) \quad (1)$$

$$P_{\mathrm{sw\_}I} = \frac{1}{\pi} \cdot f \cdot \left(\frac{I_c}{I_{\mathrm{rated}}}\right) \cdot \left(\frac{V_{cc}}{V_{\mathrm{rated}}}\right) \times (E_{\mathrm{on}} + E_{\mathrm{off}}) \quad (2)$$

$$P_{\mathrm{cond\_}D} = \sqrt{2} I_c \cdot V_F \cdot \left(\frac{1}{2\pi} - \frac{M\cos\varphi}{8}\right) + 2I_c^2 \cdot r_F \cdot \left(\frac{1}{8} - \frac{M\cos\varphi}{3\pi}\right) \quad (3)$$

$$P_{\mathrm{sw\_D}} = \frac{1}{\pi} \cdot f \cdot \left(\frac{I_c}{I_{\mathrm{rated}}}\right) \cdot \left(\frac{V_{cc}}{V_{\mathrm{rated}}}\right) \times E_{rr}. \quad (4)$$

It is assumed that the PP IGBT is operating in a pulse width modulation controlled power converter. Therefore, V_{ce} represents the voltage drop between the collector and emitter, i_{ce} represents the collector current, M represents the modulation index of 0.8, $\cos\varphi$ represents the power factor of 0.85, E_{on} represents the turn-on energy, and E_{off} represents the turn-off energy. For the FRD chip, V_F represents the voltage drop and E_{rr} represents the recovery energy.

The silicon chip junction temperature is one of the most important parameters because it affects both the on-state voltage drop and switch energy. The influence of the junction temperature on the electrical characteristics of the IGBT and FRD chips is considered in the calculation formulas to make them more accurate. As shown in (5) to (8), the relationship between the electrical parameters and junction temperature is approximately linear. T_j is the silicon chip junction temperature, which ranges from 25 to 125 °C. K_v represents the relationship between the on-state voltage drop and junction temperature, and K_r denotes the on-state resistance parameter coupled with the junction temperature. Subscripts I and D denote the IGBT and FRD chips, respectively. K_{on} and K_{off} express the influence of the junction temperature on the turn-on and turn-off energies, respectively. K_{rr} denotes the recovery energy coefficient. Those parameters, coupled with junction temperature shown in the formulas, could be calculated with a datasheet. The IGBT and FRD chips used in this paper for the power dissipation calculation and experiments are 3300 and 3300 V/100 A, respectively

$$P_{\mathrm{cond\_I}} = \sqrt{2} I_c \cdot \left(\frac{1}{2\pi} + \frac{M\cos\varphi}{8}\right) \times \left[V_{ce(25\,^\circ\mathrm{C})} + K_{v\_I}(T_{j\_I} - 25\,^\circ\mathrm{C})\right] + 2I_c^2 \cdot \left(\frac{1}{8} + \frac{M\cos\varphi}{3\pi}\right) \times \left[r_{ce(25\,^\circ\mathrm{C})} + K_{r\_I}(T_{j\_I} - 25\,^\circ\mathrm{C})\right] \quad (5)$$

$$P_{\mathrm{sw\_I}} = \frac{1}{\pi} \cdot f \cdot \left(\frac{I_c}{I_{\mathrm{rated}}}\right) \cdot \left(\frac{V_{cc}}{V_{\mathrm{rated}}}\right) \times \left[E_{\mathrm{on}(25\,^\circ\mathrm{C})} + K_{\mathrm{on}} \cdot (T_{j\_I} - 25\,^\circ\mathrm{C}) + E_{\mathrm{off}(25\,^\circ\mathrm{C})} + K_{\mathrm{off}} \cdot (T_{j\_I} - 25\,^\circ\mathrm{C})\right] \quad (6)$$

$$P_{\mathrm{cond\_D}} = \sqrt{2} I_c \cdot \left(\frac{1}{2\pi} - \frac{M\cos\varphi}{8}\right) \times \left[V_{F(25\,^\circ\mathrm{C})} + K_{v\_D}(T_{j\_D} - 25\,^\circ\mathrm{C})\right] + 2I_c^2 \cdot \left(\frac{1}{8} - \frac{M\cos\varphi}{3\pi}\right) \times \left[r_{F(25\,^\circ\mathrm{C})} + K_{r\_D}(T_{j\_D} - 25\,^\circ\mathrm{C})\right] \quad (7)$$

$$P_{\mathrm{sw\_D}} = \frac{1}{\pi} \cdot f \cdot \left(\frac{I_c}{I_{\mathrm{rated}}}\right) \cdot \left(\frac{V_{cc}}{V_{\mathrm{rated}}}\right) \times \left[E_{rr(25\,^\circ\mathrm{C})} + K_{rr} \cdot (T_{j\_D} - 25\,^\circ\mathrm{C})\right]. \quad (8)$$

B. Thermal Model

Natural convection within PP IGBTs is generally neglected because it approximately acts as a vacuum. Thermal radiation is also considered to be insignificant as long as the temperatures are less than approximately 700 K [12]. Therefore, only thermal conduction is considered in this paper, and the basic differential formula of the PP IGBT is shown in (9); ρ is the material density, C_p is the constant pressure specific heat, t is the time, k is the thermal conductivity, and Q is the volumetric heat source

$$\rho \cdot C_p \cdot \frac{\partial T}{\partial t} - \nabla \cdot (k \cdot \Delta T) = Q. \quad (9)$$

This paper mainly focuses on the temperature distribution and its influence on the pressure distribution within PP IGBTs. As a result, the influence of external conditions on the junction temperature is not considered. The boundary conditions for the thermal model are set up as follows. The temperatures of the collector and emitter pole outer faces (case temperature) have been set to 60 °C with the assumption that the external water cooling system can sustain the case temperature as constant. The heat generation in the active area (shown in Fig. 3) of the IGBT/FRD chips is set as the IGBT/FRD chip power dissipation based on the power dissipation model. Furthermore, to make the thermal model more accurate, the thermal contact resistance between specific layers within PP IGBTs is obtained by a theoretical model and verified by the experimental result [13].

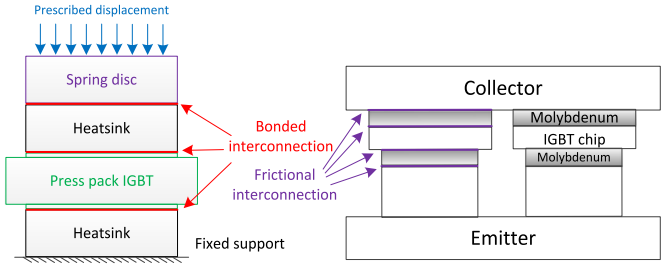

Fig. 5. Boundary conditions of the mechanical model.

C. Mechanical Model

In the application of PP IGBTs, a force spreader is used to transmit the clamping force to the heatsink and then transfer from the heatsink to the surface of the PP IGBTs. A disc spring, usually change several millimeters under the clamped phase, is needed to compensate for the physical movements, usually several micrometers, during the process of clamping and thermal expansion. To approximate to the working conditions, a prescribed displacement, which is equivalent to the rated clamping force of 70 kN, is applied to the disc spring on the surface of the heatsink of the PP IGBT collector side. A fixed support is placed on the surface of the heatsink of the PP IGBT emitter side. The simplified diagram of the boundary conditions for the mechanical model is shown in Fig. 5. The mechanical model should also consider the frictional interconnections among the different layers. The interconnections between heatsinks and PP IGBT are set as the bonded interconnection, and the interconnections between multilayers within PP IGBT are set as a frictional contact. A friction coefficient of 0.5 is assumed for the contact layers within the PP IGBT [6], [14] because the friction coefficient has a little influence on the pressure distribution [7].

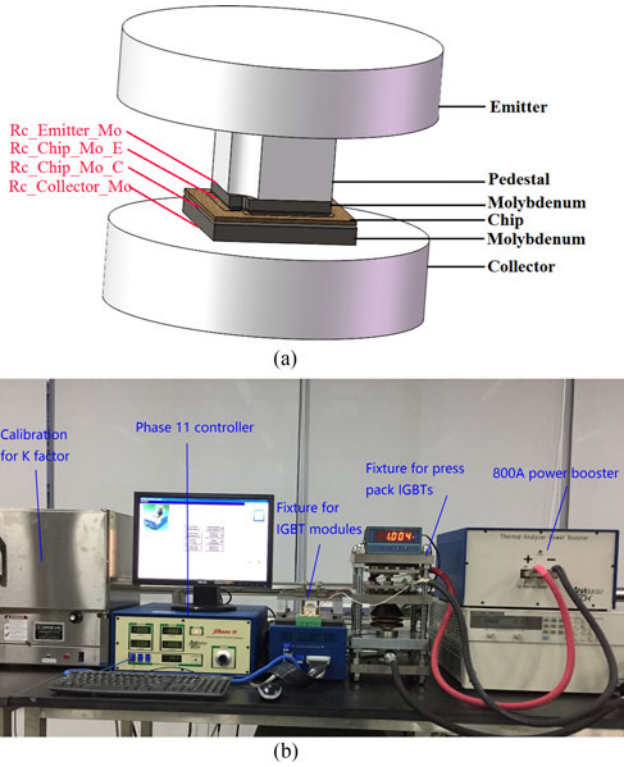

Fig. 6. Structure diagram of the IGBT submodule and thermal contact resistance test bench. (a) Single IGBT submodule diagram. (b) Thermal resistance test bench.

D. Coupling Variable for a Multiphysics Model

As shown in Fig. 4, the FEM multiphysics model proposed in this paper is a fully directly cocoupled multiphysics field with coupling variables. The most important coupling variable for the thermal and mechanical models is the thermal contact resistance. Additionally, the variable for the power dissipation and mechanical models is the electrical contact resistance. Both the electrical and thermal contact resistances are measured or calculated through a single IGBT and FRD chip submodule.

1) Thermal Contact Resistance: Thermal contact resistance between multilayers within PP IGBTs accounts for approximately 50% of the total thermal resistance [10] and is mainly influenced by the clamping force and temperature [13]. Therefore, thermal contact resistance must be considered in the thermal model to make it more accurate and to indicate the relationship between the thermal and mechanical models. The interface specific thermal contact resistance can be experimentally determined by measuring the temperature drop across the contact interface. Another possibility is to use a theoretical or semiempirical model to calculate the thermal contact resistance. Single IGBT and FRD chip submodules are fabricated to more explicitly explain the thermal contact resistance between specific layers. Additionally, the thermal contact resistance is analyzed using the semiempirical model proposed by Bahrami *et al.* [15] and the key parameters of this model are obtained by the experimental results. Finally, all the simulation results are verified by experimental results [13]. The structure diagram of the single IGBT submodule and test bench is shown in Fig. 6.

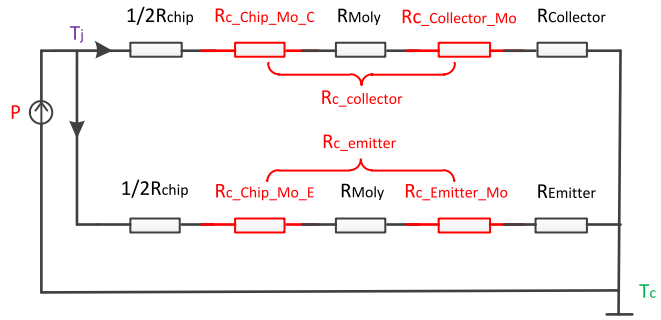

Fig. 7. Equivalent thermal network of the single IGBT submodule.

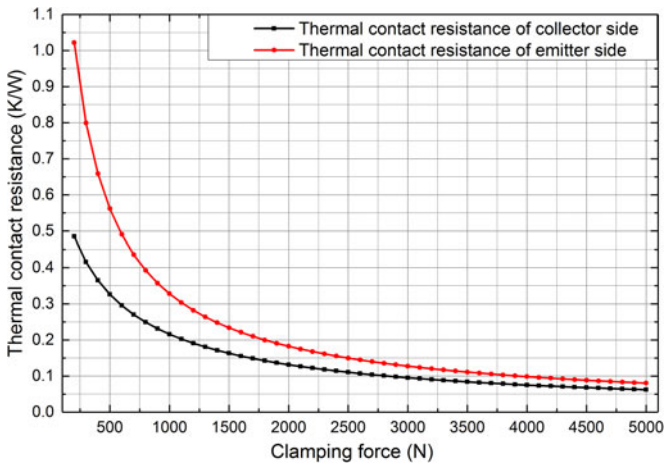

Fig. 8. Relationships between the thermal contact resistance and clamping force of the single IGBT chip submodule.

Fig. 7 gives the equivalent thermal network of a single IGBT submodule. The thermal contact resistance of the same side is connected in series, such as with the collector and emitter sides. As a result, the thermal contact resistance of the same side can be equivalent to a single thermal contact resistance for simplification. The relationships between the clamping force and the thermal contact resistance of both sides of the IGBT chip submodule are shown in (10) and (11), respectively. The relationship is obtained by the semiempirical model and verified by the experimental results, as shown in Fig. 8

$$R_{c(c)\_I} = 0.0738 + 0.474 * e^{-0.0011*F} \tag{10}$$

$$R_{c(e)\_I} = 0.111 + 1.141 * e^{-0.001*F}. \tag{11}$$

Based on the picture and formulas, we can see that the thermal contact resistances between the collector and emitter sides differ, and the reasons for this difference include the distinction of the contact area of the two sides and their differences in the IGBT chip surface roughness (measured surface roughness—collector side: Ra 0.436 and emitter side: Ra 0.842). In the same way, the thermal contact resistance of the single FRD chip submodule is also obtained and shown in Fig. 9 and the following equations:

$$R_{c(c)\_D} = 0.07584 + 0.50055 * e^{-0.00118*F} \tag{12}$$

$$R_{c(e)\_D} = 0.09469 + 0.86495 * e^{-0.00151*F}. \tag{13}$$

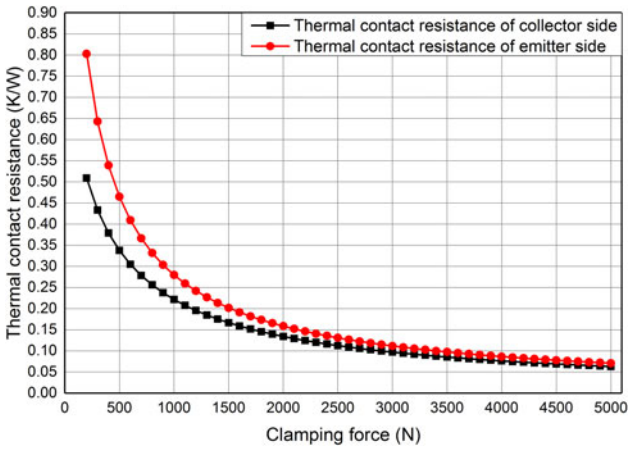

Fig. 9. Relationships between the thermal contact resistance and clamping force of the single FRD chip submodule.

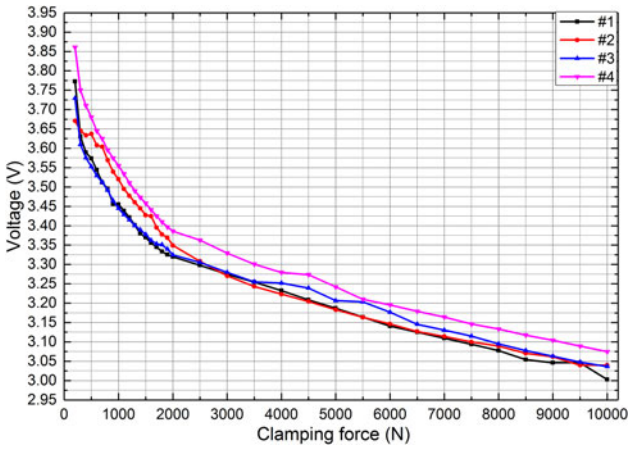

Fig. 10. Relationship between the voltage drop of the IGBT submodule and clamping force with rated current at 50 A.

2) Electrical Contact Resistance: The electrical contact resistance between multilayers within PP IGBTs is also sensitive to the clamping force, which is the same as the thermal contact resistance. Additionally, direct measurement is quite difficult because the size of the components is very small and there is no space to place the probes. However, unlike the connection relationship of the thermal contact resistance in a single IGBT chip submodule, the electrical contact resistance is connected in series from the collector to emitter sides. Therefore, the relationship between the electrical contact resistance and clamping force will be clarified as the relationship between the total electrical resistance and clamping force is given. The on-state characteristic of four single IGBT and FRD chip submodules under different clamping forces is measured through the Aglient B1505A. The relationship between the on-state voltage drop of the IGBT submodule with a rated current at 50 A and clamping force is revealed in Fig. 10. The clamping force ranges from 200 N to 10 kN.

As the data shown in Fig. 10, the change trend is the same for these IGBT chip submodules. However, the amplitude differs because of the inconsistency of these IGBT chips. The on-state

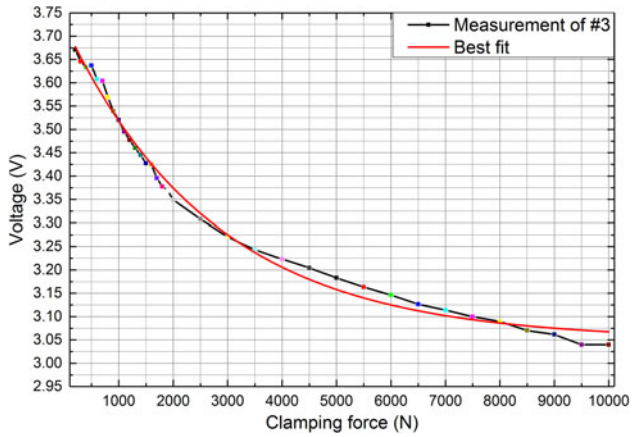

Fig. 11. Best fit of the #3 IGBT submodule measurement data at 50 A.

voltage drop decreases as the clamping force increases, even up to 10 kN per single IGBT chip submodule. The relationship may be divided into two portions, one for 200 N to 2 kN and the other for 2 kN to 10 kN. The on-state voltage drop mainly decreases in the forepart because of the electrical contact resistance between multilayers. The electrical contact resistance decreases with the clamping force increase. However, the relationship between the voltage drop and clamping force in the second portion may be the IGBT chip characteristic, which is changed with the clamping force. The electrical contact resistance may not change enough under such a high clamping force to alter the on-state voltage drop.

This paper mainly focuses on the current distribution rather than on an accurate calculation of the current. As a result, the data in the #3 submodule are selected for analysis. The best fit of the measurement is shown in Fig. 11, and the formula is given as

$$V_I(F) = 3.05 + 0.6754 * 0.99963\hat{}F. \tag{14}$$

The relationship between the electrical resistance and the clamping force could be obtained from (14) and Ohm's law with the assumption that the bulk electrical resistance is constant with the clamping force variation. To directly couple the mechanical model with the power dissipation model, the relationship between the collector current and clamping force is acquired under a rated clamping force of 1 kN and is set as the input parameter of the power dissipation model, which is shown as

$$I_I(F) = \frac{175.84}{3.05 + 0.6754 * 0.99963\hat{}F}. \tag{15}$$

Furthermore, the relationship between the voltage drop of the single FRD chip submodule and clamping force is also measured through the Aglient B1505A and is shown in Fig. 12. In the same way, the experimental result of the #3 FRD submodule is also selected to represent the relationship, which is shown in Fig. 13. The relationship between the current and clamping force is transformed through (16) and shown in (17)

$$V_D(F) = 2.284 + 2.398 * 0.99686\hat{}F \tag{16}$$

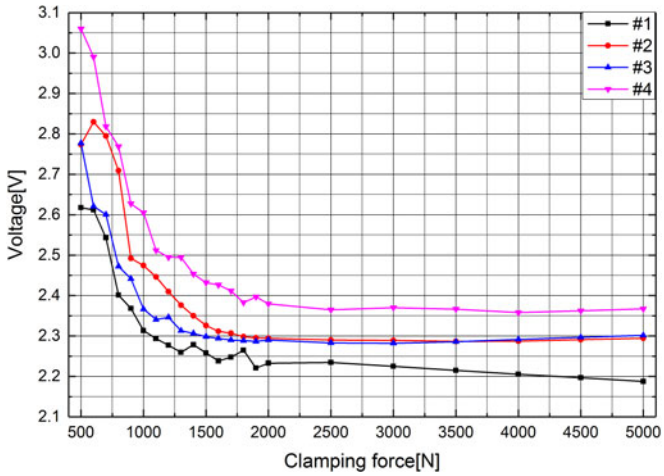

Fig. 12. Relationship between the voltage drop of the FRD submodule and clamping force with the rated current at 100 A.

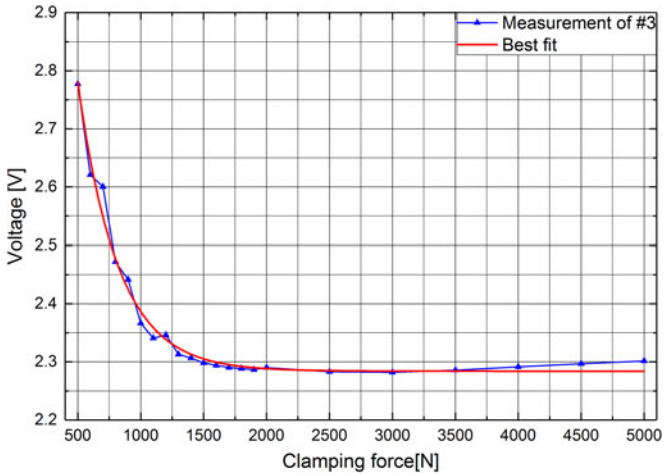

Fig. 13. Best fit of the #3 FRD submodule measurement data at100 A.

$$I_D\,(F) = \frac{238.73}{2.284 + 2.398 * 0.99686\hat{}F}. \tag{17}$$

III. Simulation Results

In this paper, the collector current, temperature, and pressure distributions within the studied PP IGBT are analyzed based on the FEM multiphysics model coupled with the electrical, thermal, and mechanical fields. Most importantly, the influence of the temperature on the pressure distribution is discussed and a comparison with the clamping phase is made.

A. Clamping Phase

The clamping phase in this paper is the state that the studied PP IGBT is only clamped by prescribed displacement, and the heating phase in the next section is the state that the clamped PP IGBT is heated up with the collector current to approximate its working state. The time scale for the heating phase is steady state. The pressure distribution within the studied PP IGBT with the clamping phase is simulated for comparison with the heating phase. Fig. 14 shows the pressure distribution between the molybdenum plate and the IGBT chip on the emitter side. The results show that the pressure distribution is relatively uniform among the silicon chips within the studied PP IGBT. The pressure of the external chips is relatively smaller than the chips located in the center. One reason is that the collector electrode is warped under the external clamping force, as shown in Fig. 15. The deformation is the cross-sectional view of the

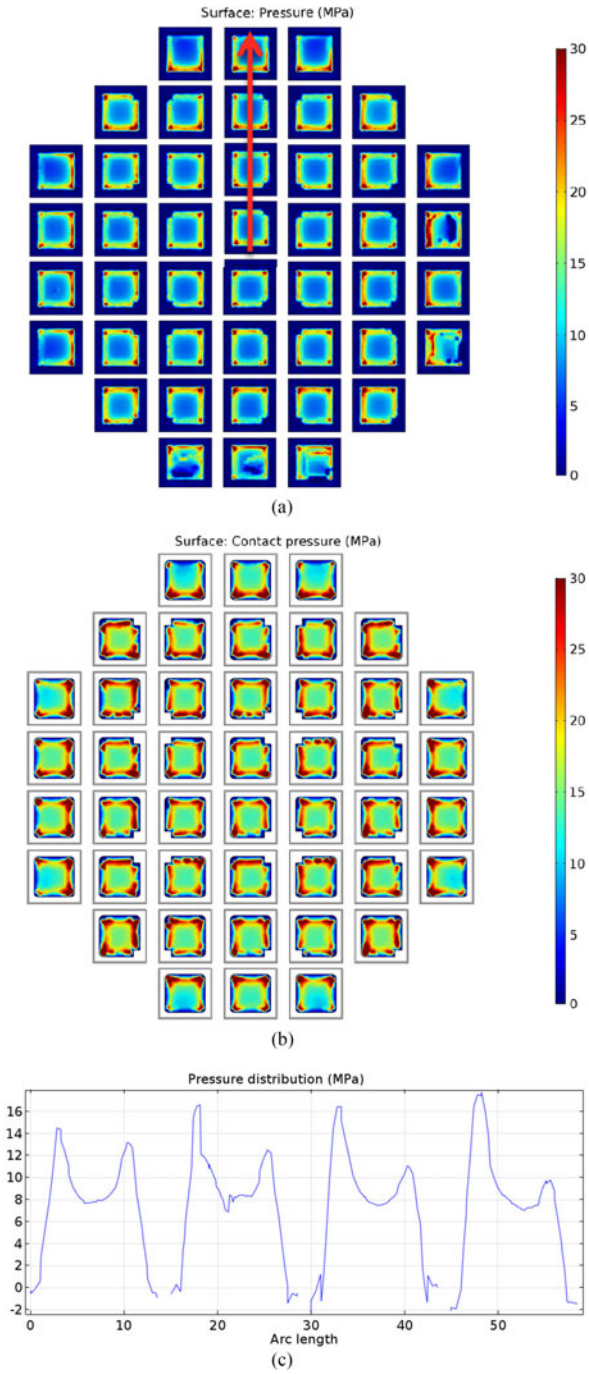

Fig. 14. Pressure distribution between molybdenum and the IGBT chip on the emitter side. (a) Pressure distribution. (b) Contact pressure distribution. (c) Pressure distribution of the extracted path.

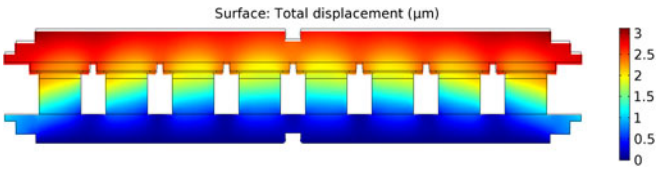

Fig. 15. Schematic of the deformation (scaling factor: 200).

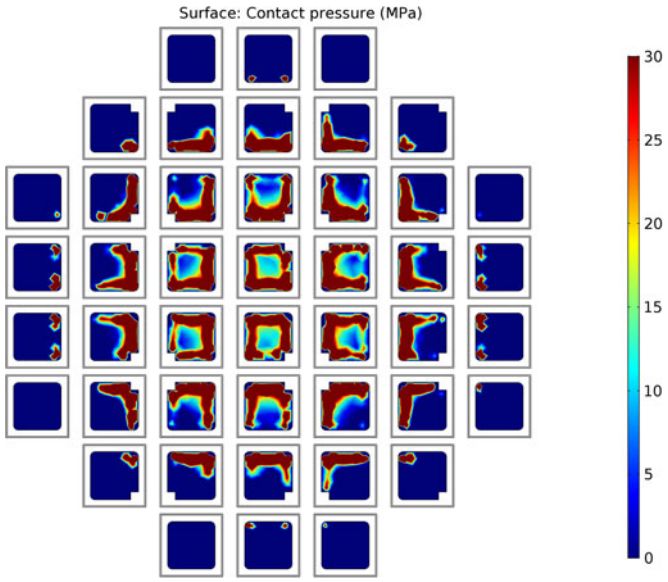

Fig. 16. Pressure distribution between molybdenum and the IGBT chip on the emitter side.

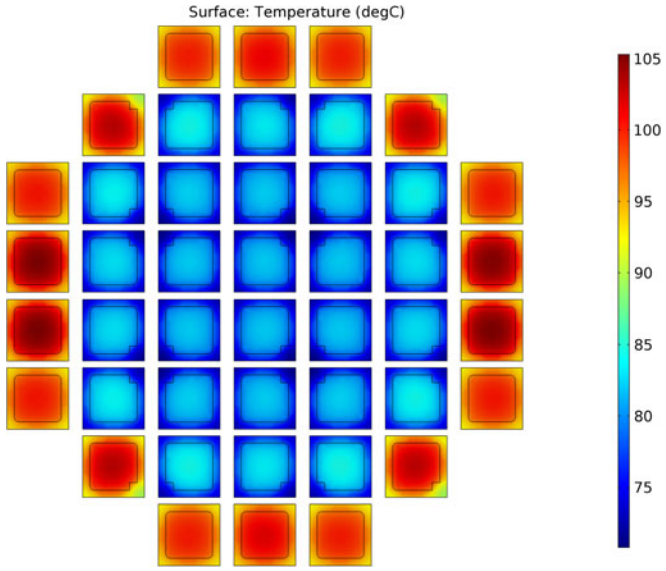

Fig. 17. Temperature distribution within the PP IGBT.

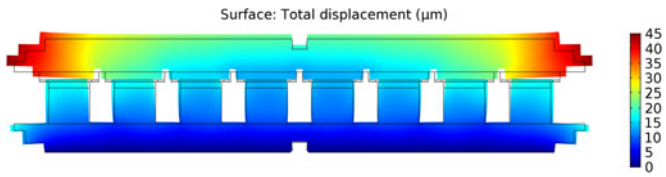

Fig. 18. Schematic of the deformation (scaling factor: 50).

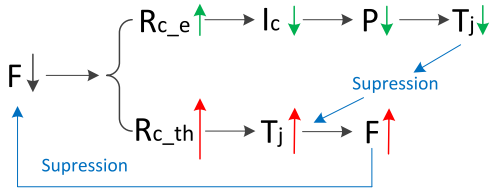

Fig. 19. Diagram of the temperature change.

studied PP IGBT and the central axis is the red line shown in Fig. 14(a). However, the pressure is concentrated in the area between the active and terminal areas of a single silicon chip. The pressure distribution along the red axis is extracted and is shown in Fig. 14(c). The pressure in the border between the active and terminal areas is much higher than the value in the active area, which is the reason why the chip broke in this area when too much pressure was applied, as shown in Fig. 2(a).

B. Heating Phase

All components in the PP IGBTs are sensitive to temperature, and their characteristics change with the temperature variation. The pressure distribution within the PP IGBTs is also affected by the thermal stress generated by the IGBT chips. The contact pressure and junction temperature distributions are shown in Figs. 16 and 17, respectively.

The simulation results show that the pressure distribution is extremely uneven within the PP IGBT and is mainly concentrated in the center. The pressure at the edge of the PP IGBT is very low and there was loss of contact. This will greatly increase the thermal contact resistance and junction temperature (shown in Fig. 17), which eventually leads to thermal damage, as shown in Fig. 2(b). This phenomenon is caused by the thermal expansion generated by the high temperature of the silicon chip's power dissipation, and the thermal expansion significantly warps the collector electrode, as shown in Fig. 18. Furthermore, the extremely nonuniform pressure distribution in a single silicon chip will also accelerate the mechanical damage at the corner between the active and terminal areas, as shown in Fig. 2(a).

The silicon chip temperature at the edge of the PP IGBT is much higher than that in the center, and there is a lower difference in the center. One reason is that the thermal contact resistance between multilayers has a significant influence on the temperature distribution. As shown in Fig. 19, with the assumption that one of the IGBT chip's clamping forces F decreases, the electrical and thermal contact resistances simultaneously increase. However, the amplitude of the augmentation differs and the proportion of the thermal contact resistance is much higher than the electrical contact resistance. The collector current I_c decreases as the electrical contact resistance R_{c_e} increases. The power dissipation P and junction temperature T_j also decrease. However, the junction temperature T_j of the IGBT chip greatly increases with increase in the thermal contact resistance R_{c_th}. Finally, the junction temperature T_j still has significant augmentation with consideration for the influence on both the electrical and thermal contact resistances.

TABLE I
SIMULATION RESULTS OF SELECTED CHIPS UNDER THE HEATING PHASE

No	F (N)	I_c/I_F (A)	P (W)	T_j (°C)
#2	84.841	86.932	82.781	101.65
#3	2301.3	50.095	108.83	83.908
#8	2949.6	50.991	110.34	82.790
#13	3072.5	51.146	110.63	82.684

TABLE II
AVERAGE CLAMPING FORCE COMPARISON

No	Rated (N)	F (N)		Deviation (%)	
		Case 1	Case 2	Case 1	Case 2
#2	1660	1596.3	84.841	−3.84	−94.89
#3	1558	1549.2	2301.3	−0.56	47.71
#8	1558	1569.1	2949.6	0.71	89.32
#13	1558	1577.8	3072.5	1.27	97.21

The average clamping force F, collector current I_C/I_F, power dissipation P, and junction temperature T_j of a FRD chip (#2) and three IGBT chips (#3, #8, and #13) located in the axis are extracted (marked with a red block in Fig. 1) and listed in Table I. The average clamping forces of those 30 IGBT chips and 14 FRD chips are 2242.5 and 195.19 N, respectively. The pressure of the FRD chips surrounding the PP IGBT is much lower than the IGBT chips. Among the selected chips, the maximum clamping force is 3072.5 N (#13), and the minimum is only 84.841 N (#2). The difference reaches 2987.66 N. The maximum junction temperature is 101.65 °C (#2), which is almost 18.97 °C higher than the other chips because the clamping force is much lower than for other chips.

The comparison of the average clamping force and the deviation between the heating and clamping phases is shown in Table II. Case 1 describes the clamping phase and case 2 describes the heating phase. The clamping force distribution within the PP IGBT with the clamping phase is much more uniform than for the heating phase. The rated clamping force of the FRD chips is slightly higher than IGBT chips because the contact area is larger than for the IGBT chips.

IV. EXPERIMENTAL DETAILS

Based on the simulation results, we can see that the pressure distribution in the heating phase differs from the clamping phase, and the junction temperature is extremely uneven. An experiment was performed to identify the pressure distribution and mechanical model proposed in this paper. All components of the PP IGBTs are too small; for example, the silicon chips are smaller than 0.5 mm and the components are encapsulated in a ceramic housing, as shown in Fig. 1. Therefore, no space is available to place a probe/detector for the temperature or current measurement. Methods for the assessing junction temperature or its distribution measurement are limited, including the use of a fibre cable or thermal camera. Therefore, only the pressure distribution within the PP IGBTs was measured in this paper.

Fuji prescale film is the most commonly used material to precisely measure the pressure, pressure distribution, and pressure balance. Red patches appear on the film wherever contact pressure is applied and the colour density varies according to the differing contact pressure levels. The prescale film pressure ranges from 0.05–300 MPa and is divided into seven levels. The pressure level of 0.5–10 MPa is selected to measure the pressure distribution within PP IGBTs according to the recommended clamping pressure [3]. However, the prescale film is electrically and thermally insulated so only the pressure distribution in the clamping phase can be verified. The pressure distribution test bench is shown in Fig. 20(a) and contains the clamping fixture, clamping force sensor, the studied PP IGBT, etc.

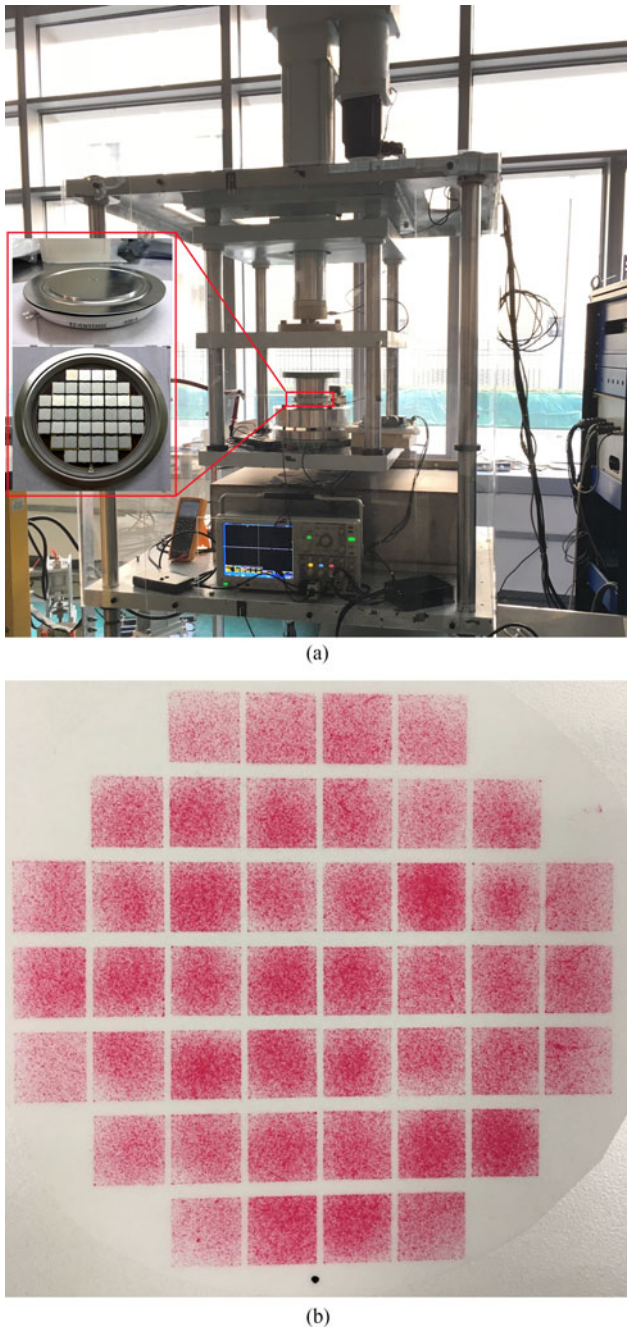

Fig. 20. Pressure distribution test bench and experimental result. (a) Test bench. (b) Experimental pressure distribution.

The pressure distribution within the PP IGBTs is affected by many external and internal factors, such as the external clamping

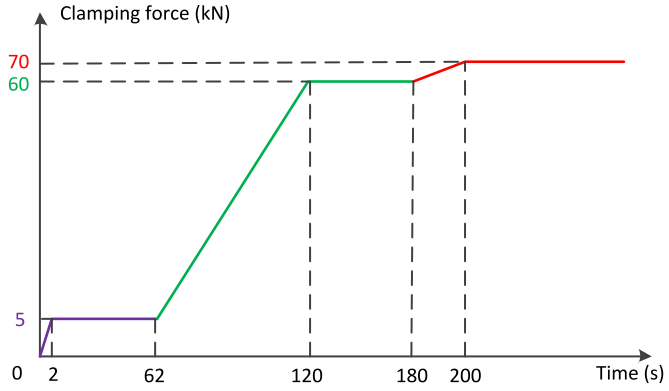

Fig. 21. Mission profile of the applied clamping force.

system, machining accuracy of components to form a submodule, etc. A sphere system is introduced in this test bench to adjust the surface flatness and ensure clamping force uniformity on the surface of the PP IGBT. At the same time, the difference in the height of each submodule also greatly affects the pressure distribution. However, it is impossible to ascertain that the height of all submodules within the PP IGBTs is maintained as the same in the experiment. All components to form the submodule are strictly selected to match each other using a high-precision height tester (Mitutoyo 518-314A-21) and the height of all submodules is strictly controlled. Finally, the maximum height difference of all submodules within PP IGBTs is kept smaller than 10 μm. Furthermore, the mission profile of the clamping force is also important for experimental results because the Fuji pressure film actually measures the peak pressure not the final pressure. The mission profile of the clamping force for the studied PP IGBT in this paper is shown in Fig. 21. It can be divided into three parts. First, a relative small value of the clamping force is applied on the studied PP IGBTs to make all components contacted and this state will last for about 1 min to make the clamped phase stable, and then, the clamping force is increased slowly to approximate the needed value for about 1 min. Finally, the needed clamping force is applied more slowly on the studied PP IGBT as shown in figure. Meanwhile, the fluctuation of the clamping force during the clamping phase have a little influence on the pressure distribution because it mainly affects the total clamping force and the pressure distribution will not change much. Therefore, this ensures that the experimental results of the Fuji pressure film can reflect the actual pressure distribution within PP IGBTs after it is clamped.

Because it is impossible to obtain the pressure distribution in the heating phase, the experimental result in the clamping phase is used to verify the mechanical model and its boundary conditions, as shown in Fig. 20(b). The pressure distribution is relatively uniform, except that several submodules are slightly higher than others such that the red colour is slightly deeper than other submodules.Additionally, the experimental result agrees well with the simulation result.

According to the experimental result in the clamping phase, the mechanical model and boundary conditions proposed in this paper are sufficiently accurate. Additionally, the simulation results in the heating phase are accurate.

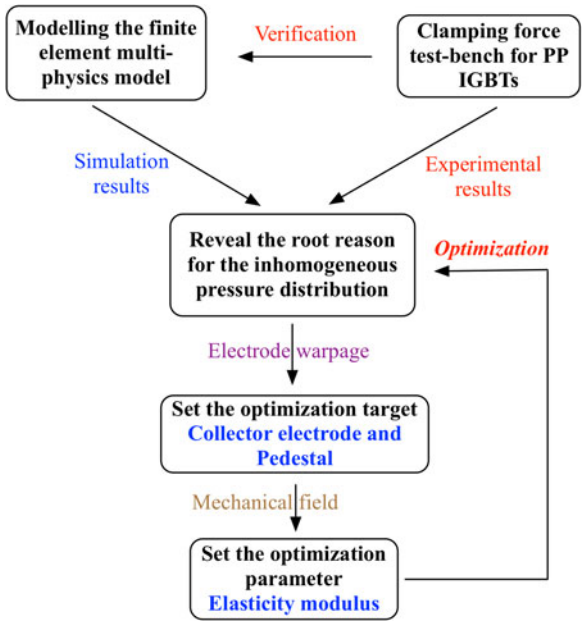

Fig. 22. Flowchart of the optimization.

TABLE III
SIMULATION RESULTS OF THE SELECTED CHIPS COMPARISON WITH THE HEATING PHASE

No		#2	#3	#8	#13
F (N)	Basic	84.841	2301.3	2949.6	3072.5
	Electrode	611.07	2247.9	2510.5	2453.4
	Pedestal	844.62	1964.9	2505.9	2671.6
I_c/I_F (A)	Basic	86.932	50.095	50.991	51.146
	Electrode	108.81	50.205	50.617	50.530
	Pedestal	105.65	49.885	50.775	51.020
P (W)	Basic	82.781	108.83	110.34	110.63
	Electrode	101.17	110.88	111.57	111.45
	Pedestal	90.967	108.76	110.14	110.55
T_j (°C)	Basic	101.65	83.908	82.790	82.684
	Electrode	100.72	91.300	90.716	90.936
	Pedestal	88.017	85.342	83.709	83.406

V. OPTIMIZATION

According to the simulation and experimental results, we can see that the pressure distribution within the PP IGBTs in the clamping phase is uniform through controlling the external and internal impact factors. However, the pressure distribution is changed when the chips are heated during its working phase. At the same time, the junction temperature is significantly affected by the nonuniform pressure distribution, which is caused by thermal contact resistance. Additionally, the nonuniform junction temperature eventually affects the electrical characteristics and reliability of silicon chips. As shown in Figs. 15 and 18, the root cause of this nonuniform pressure and junction temperature distribution is the warpage of the collector electrode. Meanwhile, the pedestal on the emitter side shown in Fig. 1(a) is too hard to compensate for the displacement caused by thermal stress in the heating phase. Therefore, optimization of the collector electrode and pedestal is proposed to improve the pressure distribution in both the clamping and heating phases based

TABLE IV
SIMULATION RESULTS COMPARISON FOR THE CLAMPING PHASE

	Clamping force (N)				Deviation (%)			
	Rated	Basic	Electrode	Pedestal	Rated	Basic	Electrode	Pedestal
#2	1660	1596.3	1628.9	1609.2	–	−3.84	−1.87	−3.06
#3	1558	1549.2	1551.9	1572.2	–	−0.56	−0.39	0.91
#8	1558	1569.1	1518.0	1581.4	–	0.71	−2.57	1.50
#13	1558	1577.8	1491.0	1576.5	–	1.27	−4.30	1.19

on the simulation results in this paper. The flowchart of the optimization for the pressure distribution within PP IGBTs is shown in Fig. 22.

As shown in Fig. 22, we can reveal the root reason for the inhomogeneous pressure distribution within PP IGBTs through the simulation and experimental results, and then, the collector electrode and pedestal are set as the optimization target because the root reason for the inhomogeneous pressure distribution is the warpage of the collector electrode and the pedestal is also too hard to compensate the displacement caused by the thermal stress. As the elasticity modulus is the most important parameter in mechanical field, it is, therefore, set as the optimization parameter to optimize the pressure distribution within PP IGBTs. The multiphysics model and its boundary conditions for optimization is the same as before. Only the elasticity modulus of the collector electrode and pedestal is changed to analyze its influence on the pressure distribution. During this simulation, the spring force is strictly controlled through the prescribed displacement as stated in the mechanical model section. The spring disc matches with the prescribed displacement to ensure the needed spring force. Generally, the displacement caused by the thermal expansion is several micrometers and the spring disc is selected to change several millimeters under clamped state in order to compensate for the physics movements during the process of clamping and thermal expansions. Thus, this ensures the needed clamping force for PP IGBTs. It can be expected that a harder collector electrode, such as molybdenum, can reduce the warpage and eventually improve the pressure distribution. Meanwhile, a softer pedestal, such as silver or even a shape memory alloy, can compensate for the displacement caused by thermal stress and improve the pressure distribution.

The average clamping force F, collector current I_c/I_F, power dissipation P, and junction temperature T_j of those selected chips in the heating phase with different methods are shown in Table III. The values from Table I are the baseline for comparison. The simulation results of the copper collector electrode replaced with molybdenum agre shown in electrode. The elastic modulus of the copper pedestal is 110 GPa, and it has been changed to 22 GPa to make it softer and compensate for the displacement caused by thermal stress. The simulation results are shown in Pedestal. Furthermore, the average clamping force in the clamping phase is also compared and shown in Table IV.

From the data, we can see that the optimization of the collector electrode and pedestal can greatly improve the pressure distribution in the heating phase. Meanwhile, the pressure distribution in the clamping phase remains uniform without significantly changing. Ideally, the shape memory alloy, such as spring, is the best selection for the displacement compensation in the heating phase to improve the pressure distribution. However, the electrical and thermal characteristics are somewhat limited. Therefore, the selection and optimization of the pedestal is a tradeoff.

VI. CONCLUSION

A FEM multiphysics model that is fully coupled with the electrical, thermal, and mechanical fields is proposed in this paper to predict the collector current, temperature, and pressure distribution within PP IGBTs based on theoretical and experimental results. The coupling variables, such as the electrical and thermal contact resistances, are measured or calculated through a single IGBT and FRD chip submodule to make the proposed multiphysics model fully and directly cocoupled. Various preliminary conclusions can be drawn based on the simulation and experimental results.

1) The high temperature generated by the silicon chips' power dissipation has a significance influence on the pressure distribution within PP IGBTs in the heating phase compared with the clamping phase. The silicon chips at the edge of the packaging have an extremely low clamping pressure and the silicon chips located in the center maybe cracked because the pressure concentred at the corner of the active area.
2) The junction temperature is also very uneven because of the pressure distribution and thermal contact resistance. The junction temperature of the silicon chips at the edge of the packaging is much higher than other chips. More attentions should pay to the silicon chips at the edge during the design process and application.
3) The mechanical model and its boundary conditions verified by the experimental results show that the multiphysics model is accurate for predicting the collector current, temperature, and pressure distribution within PP IGBTs.
4) We can see that the optimization of the pedestal is better than the electrode. However, the selection and optimization of the pedestal is a tradeoff because the electrical and thermal characteristics may be limited.

REFERENCES

[1] F. Wakeman, D. Hemmings, W. Findlay, and G. Lockwood, *Pressure* Contact *IGBT,* Testing *for* Reliability, Westcode Semiconductors, Ltd., Chippenham, U.K., Mar. 2012.

[2] C. Busca *et al.*, "An overview of the reliability prediction related aspects of high power IGBTs in wind power applications," *Microelectron. Rel.*, vol. 51, nos. 9–11, pp. 1903–1907, 1903.
[3] A. Hasmasan, C. Busca, R. Teodorescu, and L. Helle, "Electro-thermal-mechanical analysis of high-power press-pack insulated gate bipolar transistors under various mechanical clamping conditions," *IEEJ J. Ind. Appl.*, vol. 3, pp. 192–197, 2013.
[4] *Recommendations Regarding Mechanical Clamping of Press Pack High Power Semiconductors*, ABB, Zürich, Switzerland, 2004.
[5] *Application Note for Device Mounting Instructions*, Westcode Semiconductors, Ltd., Chippenham, U.K., Mar. 2012.
[6] A. Pirondi *et al.*, "Thermo-mechanical simulation of a multichip press-packed IGBT," *Solid-State Electron.*, vol. 42, no. 12, pp. 2303–2307, 1998.
[7] P. Cova *et al.*, "Power cycling on press-pack IGBTs: Measurements and thermomechanical simulation," *Microelectron. Rel.*, vol. 39, no. 6, pp. 1165–1170, 1999.
[8] T. Poller, T. Easier, M. Hernes, S. D'Arco, and J. Lutz, "Mechanical analysis of press-pack IGBTs," *Microelectron. Rel.*, vol. 52, pp. 2397–2402, 2012.
[9] T. Poller, S. D'Arco, M. Hernes, A. R. Ardal, and J. Lutz, "Influence of the clamping pressure on the electrical, thermal and mechanical behavior of press-pack IGBTs," *Microelectron. Rel.*, vol. 53, pp. 1755–1759, 2013.
[10] C. Busca, R. Teodorescu, F. Blaabjerg, L. Helle, and T. Abeyasekera, "Dynamic thermal modelling and analysis of press-pack IGBTs both at component-level and chip-level," in *Proc. 2013 39th Annu. Conf. IEEE Ind. Electron. Soc.*, 2013, pp. 677–682.
[11] A. Patel, S. Joshi, H. Chandwani, V. Patel, and K. Patel, "Estimation of junction temperature and power loss of an IGBT used in VVVF inverter using numerical solution from data sheet parameter," *Int. J. Comput. Commun. Inf. Syst.*, vol. 2, 2010, pp. 17–22.
[12] A. Bejan and D. Kraus, *Heat Transfer Handbook*. New York, NY, USA: Wiley, 2003.
[13] E. Deng *et al.*, "Optimization of the thermal contact resistance within press pack IGBTs," *Microelectron. Rel.*, vol. 69, pp. 17–28, 2017.
[14] A. Pirondi, G. Nicoletto, P. Cova, M. Pasqualetti, and M. Portesine, "Thermo-mechanical finite element analysis in press-packed IGBT design," *Microelectron. Rel.*, vol. 40, pp. 1163–1172, 2000.
[15] M. Bahrami, J. R. Culham, M. M. Yovanovich, and G. E. Schneider, "Thermal contact resistance of non-conforming rough surfaces. Part 1. Mechanical model," presented at the 36th AIAA Thermophys. Conf., Orlando, FL, USA, Jun. 23—26, 2003, Paper 2003-4197.

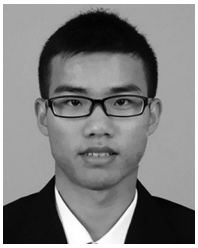

Erping Deng (M'17) was born in Hunan province, China, in 1989. He received the Bachelor's degree in electrical engineering from Harbin Institute of Technology, Harbin, China, in 2013. He is currently working toward the Ph.D. degree at the State Key Laboratory of Alternate Electrical Power System With Renewable Energy Sources, North China Electric Power University, Beijing, China.

His main research focuses on the packaging and reliability of high-voltage and high-power electronics devices.

Zhibin Zhao (M'17) was born in Hebei province, China, in 1977. He received the Ph.D. degree in electrical engineering from North China Electric Power University, Beijing, China, in 2005.

He is currently a Professor with the State Key Laboratory of Alternate Electrical Power System With Renewable Energy Sources, North China Electric Power University. His main research interests include computational electromagnetics and electromagnetic compatibility in high-power electronic devices.

Zhongkang Lin was born in Henan province, China, in 1989. He received the Master's degree in engineering mechanics from the University of Chinese Academy of Sciences, Beijing, China, in 2015.

He is currently a Research Engineer with the Global Energy Interconnection Research Institute, State Grid Corporation of China, Beijing. His main research interests include mechanical analysis and multiphysics field simulation research of high-voltage and high-power electronics devices.

Ronggang Han was born in Shaanxi province, China, in 1982. He received the Bachelor's degree in electronics science and technology from Xi'an University of Technology, Xi'an, China, in 2004.

He is currently mainly involved in power semiconductor device packaging and test.

Yongzhang Huang was born in Guangxi, China, in 1962. He received the B.S. degree in physics from the Department of Engineering Physics, Tsinghua University, Beijing, China, in 1984, and the Ph.D. degree in physics from Chinese Academy of Sciences, Beijing, in 1991.

He is currently a Professor in the Department of Electrical Engineering, North China Electric Power University, Beijing. He is also a Chinese Distinguished Expert of "thousand talents program" and the Deputy Director of the State Key Laboratory of Alternate Electrical Power System With Renewable Energy Sources, North China Electric Power University. His current research interests include advanced transmission technology and power system electromagnetic compatibility technology.